Hindawi Publishing Corporation
Journal of Nanoparticles
Volume 2014, Article ID 760712, 7 pages
http://dx.doi.org/10.1155/2014/760712

Research Article

Influence of Gas Sort on the Nucleation Region Width of Si Nanocrystal Grains Prepared by Pulsed Laser Ablation

Zechao Deng,[1,2] Lizhi Chu,[1,2] Xuecheng Ding,[1,2] Aili Qin,[1,2] Guangsheng Fu,[1,2] and Yinglong Wang[1,2]

[1] *College of Physics Science and Technology, Hebei University, Baoding 071002, China*
[2] *Key Laboratory of Photo-Electricity Information Materials of Hebei Province, Baoding 071002, China*

Correspondence should be addressed to Yinglong Wang; hdwangyl@hbu.cn

Received 19 November 2013; Accepted 15 February 2014; Published 30 March 2014

Academic Editor: Jerome Plain

We have calculated the nucleation region (NR) location of Si nanocrystal grains prepared by pulsed laser ablation (PLA) with fluence of 4 J/cm^2 in 10 Pa gas at room temperature, and ambient gases were He, Ne, and Ar, respectively. Results of calculation indicated that NR width in Ne gas was narrowest, while it was widest in He gas. Maximum mean size of grains deposited on substrates under ablated spot, which were placed horizontally, was the smallest in Ne gas. It would be attribute to more effective energy transfer during the process of collision when atomic mass of Si and ambient gas Ne are more close to each other. In this work, an additional gas flow with the same element as ambient gas was introduced, which is vertical to the plume axis at different lateral positions above ablated spot.

1. Introduction

Nanocrystal Si grain is the starting point for preparing nanostructured materials and devices on account of its unique physical properties compared with bulk Si [1–3]. During the past several decades, preparation technology of nanometer materials became increasingly mature [4–8]. Among the methods of experimental and theoretical studies about Si grains, pulsed laser ablation (PLA) is one of the most commonly used methods due to its unique advantages such as rapid thermogenic speed, high atoms concentration, and small surface contamination. However, so far, there is still a great difficulty to obtain ideal size of Si grains through PLA; the most main reason is the lack of knowledge about the mechanism of nucleation and growth processes in ambient gas, which is important for both technological application and fundamental research. On the study of nucleation of Si nanocrystal grains by PLA method, Muramoto et al. [9, 10], Geohegan et al. [11], Makimura et al. [12], and so forth have verified grains formed during ablated Si atoms transmission in inert gas by different methods. But they did not mention the nucleation condition, formation position, and growth process. In 2005, Fu et al. [13] brought forward the conception of nucleation region for the first time; the viewpoint considered that grains should nucleate and grow up simultaneously through collision between ablated atoms and background gas in the NR after nanosecond laser ablated Si crystal target, and its width decided the mean size and size consistency of grains; thus, finding out the effect degree of different parameters on the NR width becomes a key problem.

In this work, Si nanocrystal grains were prepared by PLA through introducing a vertical gas flow at three different positions relative to target; grains formed in space were deposited on the substrates that were horizontally placed under ablated spot. According to analyzing size and position distribution of grains, NR location was calculated combined with hydrodynamics model [14], nucleation division model [13], and flat parabolic motion-like in different ambient gases;

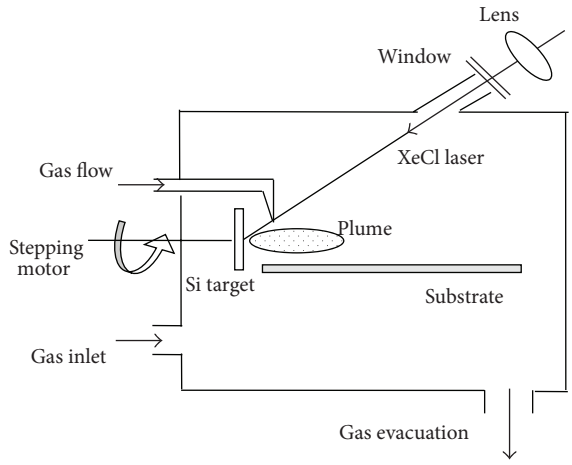

Figure 1: Schematic sketch of PLA apparatus.

the results indicate that the atomic mass of ambient gas decide the width of NR at the condition of other parameters invariable.

It is important that the gas flow introduced will promote the formed grains falling more quickly and affect its deposition location on the substrates simultaneously, but does not alter the NR location and size of grains.

2. Experimental Details

The schematic sketch of PLA apparatus was shown in Figure 1, which was different from the conventional setups [14, 15]. A XeCl excimer laser (wavelength is 308 nm and pulse duration is 15 ns) beam with repetition rate 1 Hz was focused onto a $2 \times 1\,\text{mm}^2$ rectangular spot at the surface of single crystalline Si target (resistivity is $3000\,\Omega \cdot \text{cm}$), which was rotated at 6 rpm through a stepping motor during ablation. A series of single crystalline Si (111) or glass substrates were placed under ablated spot; the vertical distance (h) between them was 2 cm. After base pressure was evacuated under 2×10^{-4} Pa, high purity (99.9999%) ambient gas was inflated into the vacuum. During the process of experiment, a beam of gas flow with the same element as ambient gas was introduced above ablated spot at positions of 1 cm, 2 cm, and 3 cm relative to target surface; the flux was 25 sccm and controlled by a flowmeter. The chamber was kept at a constant pressure of 10 Pa at room temperature using an evacuation system throughout; laser fluence was $4\,\text{J/cm}^2$.

Films deposited on glass substrates were analyzed by Raman (MKI-2000, 6328 nm) and XRD (12 kw, Cuka Radiation), while the ones deposited on Si (111) substrates were characterized by SEM (JSM-7500F).

On the base of statistical results, size and position distribution of grains on substrates are various because of different ambient gas sort, but distribution rules are similar; that is, grains form in one area apart from target, and mean size first increases and then decreases with adding distance to the target surface; position distribution of grains on the substrates with gas flow at 1 cm, 2 cm, and 3 cm in He, Ne, and Ar gas is listed in Table 1.

Table 1: Position distribution of grains on substrates with gas flow at different locations in He, Ne and Ar gas.

Location of gas flow/(cm)	Gas sort	Position of grains on substrates x/(mm)
1	He	10~58.2
	Ne	4~33.1
	Ar	5~38
2	He	10~59.2
	Ne	4~36
	Ar	5~39.8
3	He	10~61
	Ne	4~34.8
	Ar	5~45.3

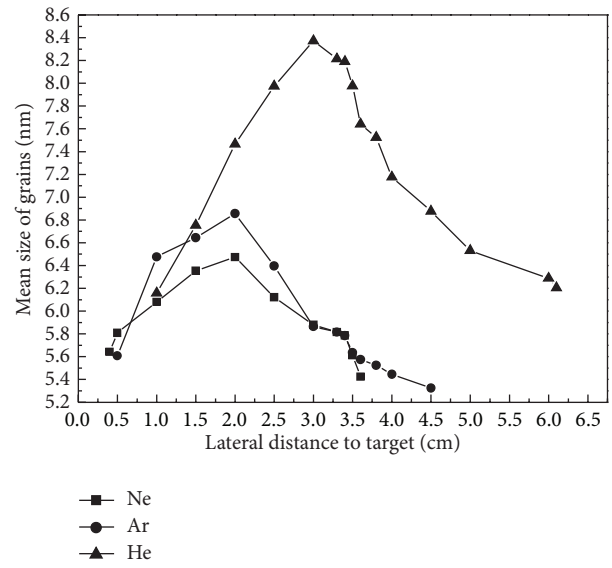

Figure 2: Distribution of grains size on substrates in different gases when gas flow is at 2 cm.

Considering the similar distribution rule, results of SEM, Raman, and XRD in Ne with gas flow at 2 cm are selected as typical representations. Grains size on substrates with different lateral distance to target when gas flow is at 2 cm is shown in Figure 2.

SEM images are shown in Figures 3(a)–3(h), corresponding to the lateral distance between the substrates and the target surface are 3.9 mm, 4 mm, 10 mm, 15 mm, 20 mm, 30 mm, 36 mm and 36.1 mm, respectively. It is obvious that no grains in (a) and (h) images, results of Raman and XRD, that verify the deposited films on glass substrates at the same position are amorphous. Images of (b) and (g) indicate that the films contain grains, which locate at 4–36 mm; that is to say, grains formed in a region scale apart from target, 4 mm and 36 mm, are in initial and end positions of grains detected on substrates. Furthermore, the statistic operation shows us

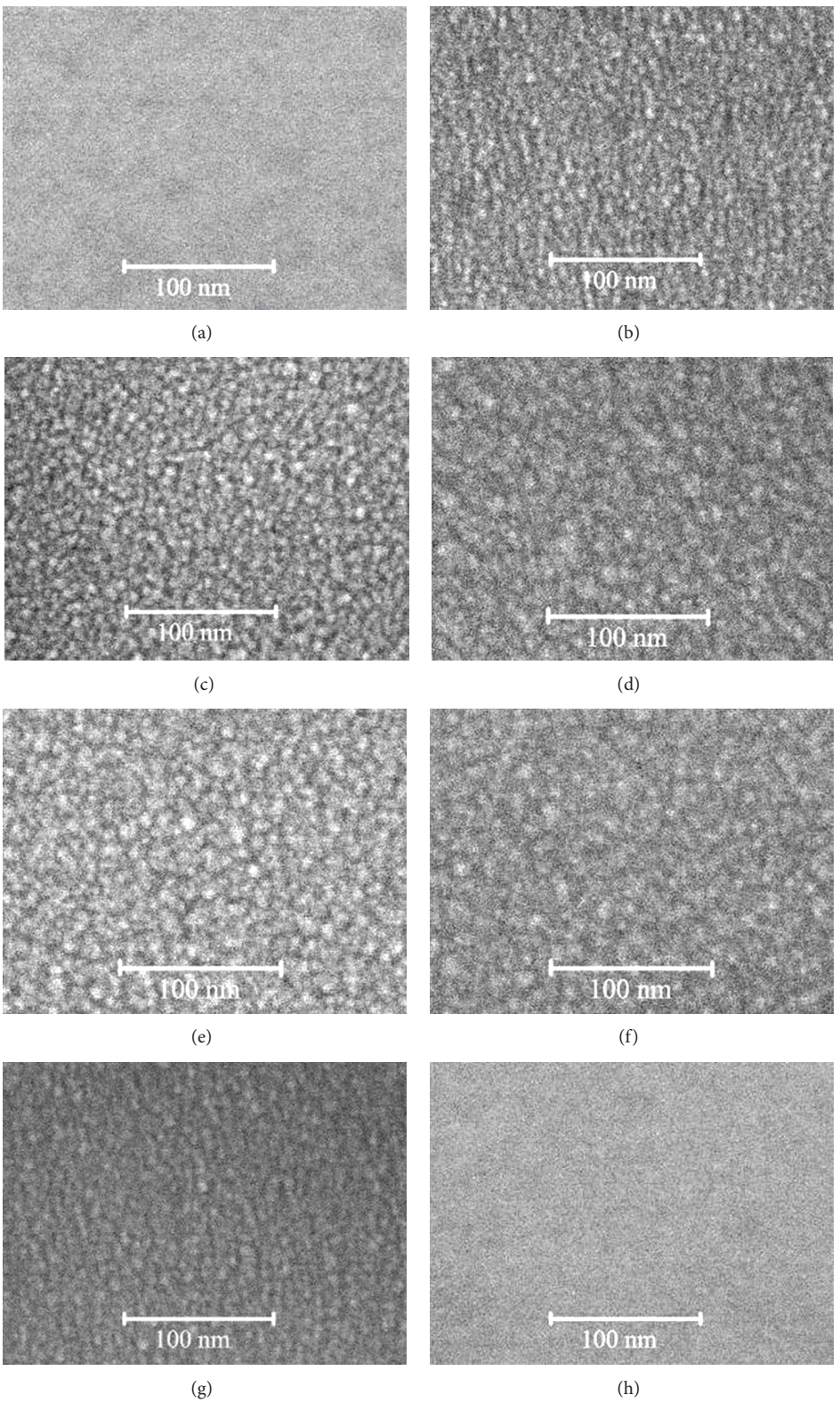

Figure 3: SEM images of samples with gas flow at 2 cm in Ne.

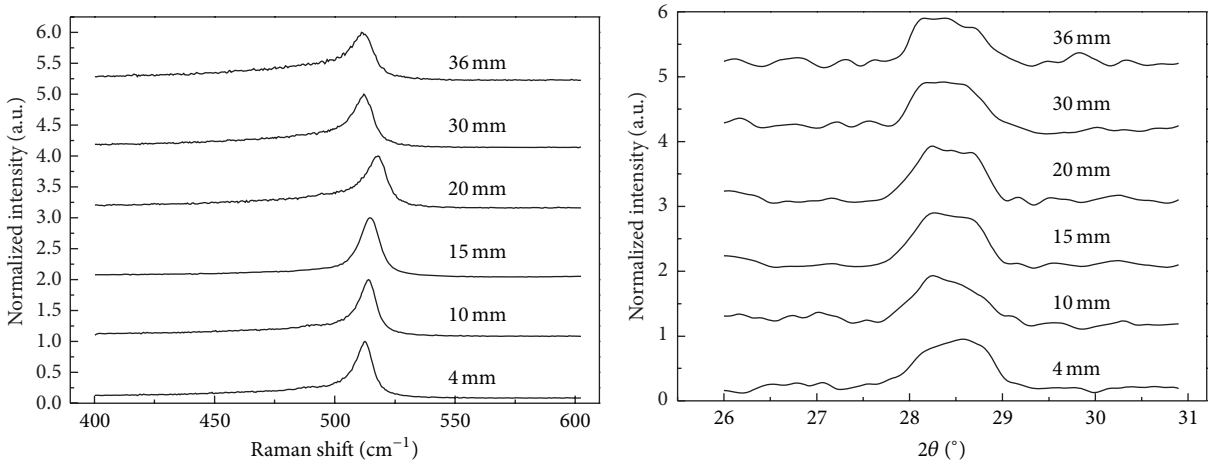

Figure 4: Raman (a) and XRD (b) spectra of samples with gas flow at 2 cm in Ne.

that mean size of grains first increases and then decreases with the addition of lateral distance to target surface.

The corresponding Raman spectra of samples on glass substrates are demonstrated in Figure 4(a); value of main peaks is 512.572 cm^{-1}, 514.051 cm^{-1}, 514.544 cm^{-1}, 517.995 cm^{-1}, 512.079 cm^{-1}, and 511.093 cm^{-1}, respectively. All values of the peaks are close to the characteristic peak value of single crystal Si, which is 520 cm^{-1}. The results prove that grains of films are crystal. Meanwhile, the main peaks first shift right and then shift left which indicates that the size of grains first increases and then decreases by equation [16] of

$$d = 2\pi\left(\frac{B}{w}\right)^{1/2} \tag{1}$$

the change rule agreement with statistic operation of SEM. In this formula, d represents diameter of grain and ω is the peak shift for grain as compared to crystal Si, $B = 2.0\,\text{cm}^{-1}\cdot\text{nm}^2$. Additionally, the peaks at around 28° of XRD in Figure 4(b) corresponding to crystal Si (111), which reveals crystalline grains, are produced too. FWHM of spectra becomes narrow first and then broadens with the increase in lateral distance, which proves that the change law of grains size is consistent with statistical results of SEM and Raman by Scherrer formula [17]

$$d = \frac{k\lambda}{\beta\cos\theta}, \tag{2}$$

where d represents diameter of grain, k is the factor of crystal figure, λ is wavelength of X-ray, and θ is diffraction angle; β is equal to $(B^2 - b_0^2)^{1/2}$, where B is the width at half tallness of diffraction peak and b_0 is the broadening factor of the instrument.

3. Numerical Calculation of Nucleation Region

The main process in this work is vapor nucleation as background gas at room temperature. Ablated plume is assumed to be limited in the cylinder with ablation spot as the base area. Ablated Si atoms spray from target after laser ablation off, energy of them wear down through elastic collision with atoms of background gas during transportation, slowing coefficient of ablated Si atom is $a_{\text{Si}} = cs_{\text{Si}}\rho/2$ [14], when supersaturation and thermal motion temperature of Si atoms reach to the threshold, the nucleation phenomenon happen [13]; c is constant, s_{Si} is collision cross of Si atom, and ρ is density of ambient gas.

According to thermodynamic equation, when ablated atom nucleates, it obeys the formula

$$kT = \frac{m_{\text{Si}}v_{\text{Si}}^2}{2} = \frac{m_\Delta v_\Delta^2}{2A^2} \tag{3}$$

and $m_{\text{Si}}/m_\Delta = (r_{\text{Si}}/r_\Delta)^3$; the formula indicates that as-formed grain possesses a certain velocity. k is Boltzmann constant, T is nucleation temperature for ablated atom, m_{Si} and r_{Si} are mass and radius of Si atom, m_Δ and r_Δ are corresponding to grain, A is energy conversion coefficient between ablated atom and grain, and v_{Si} and v_Δ are velocities of nucleated atom and formed grain, which are parallel to plume axes. As-formed grain in space will deposit on the substrates through flat parabolic motion-like under the effect of gravity and gas flow; the schematic diagram of nucleation and motion for grain is shown in Figure 5.

x_0 is the position of grain formation in space, x is its deposition location on substrates, $v_{0\text{Si}}$ is initial velocity of ablated atom, which is parallel to plume axes, v_{Si} [14] is velocity of nucleated atom at x_0, and h represents vertical distance from ablated spot to substrates, which is equal to 2 cm.

In this paper, considering the time of growth process of grain takes only tens of nanoseconds [18, 19], which can be ignored relative to the time from nucleation until depositing onto substrates, so we assume the size of grain on substrates is just the value of initial formation stage at x_0. During transportation process, collision section of Si and Ne atoms is $S_{\text{Si-Ne}} = \pi(r_{\text{Ne}} + r_{\text{Si}})^2$ and $S_{\Delta\text{-Ne}} =$

Table 2: Results of experimental measurement and theoretical calculation in different gases.

Gas sort	Atomic mass m/(u)	Position of grains on substrates x/(mm)	Max mean size d/(nm)	Nucleation location of calculation x_0/(mm)
He	4	10~61	8.4	3.6~59.8
Ne	20	4~36	6.5	2.4~34.9
Ar	40	5~45	6.9	2.7~43.2

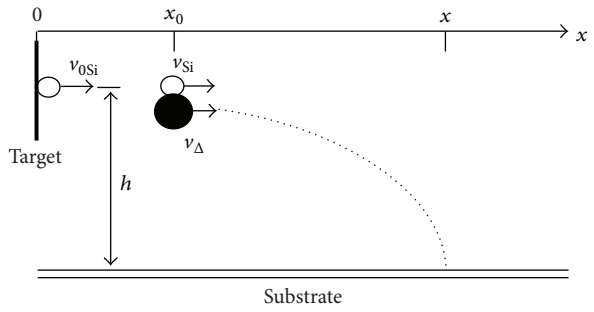

Figure 5: Schematic diagram of nucleation and motion of grain.

$\pi(r_{Ne} + r_\Delta)^2$ corresponding to grain. Slowing coefficient of grain is calculated on the basis of $a_{Si} = cs_{Si}\rho/2$, which is $a_\Delta = [r_\Delta + r_{Ne}/r_{Ne} + r_{Si}]^2 a_{Si}$; r_{Ne} is radius of Ne atom. Through hydrodynamics model of Yoshida and flat parabolic motion of grain that deposit onto substrates, formula about spatial position of grain formation is

$$x_0 = x - Av_{0Si}\sqrt{\frac{r_{Si}^3}{r_\Delta^3}}e^{-(1-A)a_{Si}x_0/m_{Si}} \times \left\{\left(-\frac{2\left(gt + v_{ag}\right)}{g} + \sqrt{\left[\frac{2\left(gt + v_{ag}\right)}{g}\right]^2 - 4\left(t^2 - \frac{2h}{g}\right)}\right) \times (2)^{-1} - \frac{\left(x_0 - x_{ag}\right)}{v_{0Si}}\right\}, \quad (4)$$

where $A = a_\Delta m_{Si}/a_{Si}m_\Delta$, v_{ag} is velocity of gas flow, t is time of grain deposit onto substrates from the height of 2 cm under effect of gravity (g) and gas flow, and x_{ag} is position of introducing gas flow. $m_{Si} = 4.67 \times 10^{-26}$ kg, $r_{Si} = 1.46$ Å, $r_{Ne} = 0.51$ Å, $v_{0Si} = 1760$ m/s [20], and $v_{ag} = 0.5$ m/s are used. Utilizing the three different positions of introduced gas flow at 1 cm, 2 cm, and 3 cm, the equation group that includes three formulas is established. The iterative calculation method is used to resolve the equation group; calculated results of NR location are 2.4 mm to 34.9 mm, so the width is 32.5 mm, and values in other gases are listed in Table 2.

4. Discussion of Results

In this work, the parameters are constant except for gas sort; distribution area of grains on substrates with different gas sort is shown in Table 2, which is widest in He, while it is narrowest in Ne; the max mean size of grains in He is maximum but minimum in Ne. In relation to the initial and last position of grains detected on substrates in Ne, positions under the other two gases shift backward. The variation feature of NR width is consistent with position distribution region of grains; that is to say, the little endian sequence for value of NR width corresponds to Ne, Ar, and He. The max mean size of grains is smallest in Ne corresponding to the narrowest NR width, which agrees with our theoretical prediction [13].

Atomic mass of Si is 28 u, and the differences between atom of He, Ne, and Ar are 24 u, 8 u, and 12 u, respectively. The above results suggest such information: when atomic mass of ambient gas is closer to Si, width of NR is narrower, and mean size of grains is smaller. On the contrary, NR width and grain size will be expanding with the larger difference of atomic mass between Si and background gas. We consider that it is contributed to energy transfer after elastic collision between atoms of ambient gas and Si. When atomic mass of ambient gas is closer to Si, the effective energy transfer is greater. On the base of thermodynamics theory, temperature of ablated atoms falls to nucleation point relatively rapid. Because the parameters of laser fluence are constant, the initial velocity and thermodynamic temperature of ablated atoms are basically fixed, and ablated atoms need less collisions before decaying down to nucleation temperature in Ne gas, which resulted in shorter transportation distance; so position of grains formation is closer to target. At the same time, there is a high nucleation rate concomitant for effective energy transfer; naturally, the number of ablated atoms decreases rapidly, and the nucleation condition is not met soon by nucleation division model, so NR width is narrower.

In this work, mean size of deposited grains first increases and then decreases with the addition of lateral distance to target, which is caused by velocity distribution rule of ablated atoms. On the base of numerical simulation, velocity of ablated atoms is Maxwell distribution, and velocity value is maximum at front of plume and minimum near plume tail; furthermore, the number of atoms with maximum and minimum velocity is less than those atoms with most probable velocity. Combined with thermodynamics formula, small velocity corresponds to lower thermal motion temperature, so temperature will reach nucleation condition [13] first through collision with ambient gas; that is to say, nucleation will happen first naturally near target (plume

tail), which have been approved by Makimura et al. [12, 21]. Taking it for granted, greater velocity corresponds to higher temperature; these atoms need to experience more collisions before nucleation, so the nucleation location is comparative farther to target surface when gas pressure is constant. For the number density [22] of atoms with the most probable velocity is much more, the nucleated grains by these atoms have bigger growth probability, which causes the mean size to be bigger. Thus the size of grains deposited on substrates first increases to a maximum and then decreases with the addition of lateral distance to target.

5. Summary

In conclusion, we have prepared Si nanocrystal grains by PLA method through an upswinged setup. Results of experiments indicate grains forming in one area apart from target, and mean size increases first and then decreases with adding distance to target surface, which is explained on the base of velocity (thermal motion temperature) and density of ablated Si atoms. NR width in He, Ne, and Ar ambient gases is calculated; the values are 56.2 mm, 32.5 mm, and 40.5 mm, respectively. The NR width is narrower when atomic mass of ambient gas is closer to Si atom. This may pave the way to further investigate concretely the nucleation and growth process for grains of Si as well as other materials in gas phase.

Conflict of Interests

The authors declare that there is no conflict of interests regarding the publication of this paper.

Acknowledgments

Project is supported by the special Foundation of State Key Development Program for Basic Research of China (2011CB612305), the NSF of Hebei Province (E2011201134 and E2012201035), and the Research Project of Colleges and University of Hebei Province (Q2012084), China.

References

[1] A. La Magna, P. Alippi, V. Privitera, and G. Fortunato, "Role of light scattering in excimer laser annealing of Si," *Applied Physics Letters*, vol. 86, no. 16, Article ID 161905, pp. 1–3, 2005.

[2] L. T. Canham, "Silicon quantum wire array fabrication by electrochemical and chemical dissolution of wafers," *Applied Physics Letters*, vol. 57, no. 10, pp. 1046–1048, 1990.

[3] G. Kurumurthy, K. S. Alee, and D. N. Rao, "Photoluminescence studies of Si/SiO_2 nanoparticles synthesized with different laser irradiation wavelengths of nanosecond pulse duration," *Optics Communications*, vol. 282, no. 17, pp. 3509–3512, 2009.

[4] T. Inokuma, Y. Wakayama, T. Muramoto, R. Aoki, Y. Kurata, and S. Hasegawa, "Optical properties of Si clusters and Si nanocrystallites in high-temperature annealed SiOx films," *Journal of Applied Physics*, vol. 83, no. 4, pp. 2228–2234, 1998.

[5] P. T. Murray and E. Shin, "Formation of silver nanoparticles by through thin film ablation," *Materials Letters*, vol. 62, no. 28, pp. 4336–4338, 2008.

[6] S. Amoruso, R. Bruzzese, X. Wang, and J. Xia, "Propagation of a femtosecond pulsed laser ablation plume into a background atmosphere," *Applied Physics Letters*, vol. 92, no. 4, Article ID 041503, 2008.

[7] A. Lorusso, V. Nassisi, G. Congedo, N. Lovergine, L. Velardi, and P. Prete, "Pulsed plasma ion source to create Si nanocrystals in SiO_2 substrates," *Applied Surface Science*, vol. 255, no. 10, pp. 5401–5404, 2009.

[8] M. S. Kim and E. S. Kim, "Fabrication of conical shape-Si particle by pulsed laser ablation," *Current Applied Physics*, vol. 9, no. 1, pp. S58–S61, 2009.

[9] J. Muramoto, Y. Nakata, T. Okada, and M. Maeda, "Influences of preparation conditions on laser-ablated Si nano-particle formation processes observed by imaging laser spectroscopy," *Applied Surface Science*, vol. 127–129, pp. 373–377, 1998.

[10] J. Muramoto, T. Inmaru, Y. Nakata, T. Okada, and M. Maeda, "Spectroscopic imaging of nanoparticles in laser ablation plume by redecomposition and laser-induced fluorescence detection," *Applied Physics Letters*, vol. 77, no. 15, pp. 2334–2336, 2000.

[11] D. B. Geohegan, A. A. Puretzky, G. Duscher, and S. J. Pennycook, "Time-resolved imaging of gas phase nanoparticle synthesis by laser ablation," *Applied Physics Letters*, vol. 72, no. 23, pp. 2987–2989, 1998.

[12] T. Makimura, T. Mizuta, and K. Murakami, "Formation dynamics of silicon nanoparticles after laser ablation studied using plasma emission caused by second-laser decomposition," *Applied Physics Letters*, vol. 76, no. 11, pp. 1401–1403, 2000.

[13] G. S. Fu, Y. L. Wang, L. Z. Chu et al., "The size distribution of Si nanoparticles prepared by pulsed-laser ablation in pure He, Ar or Ne gas," *Europhysics Letters*, vol. 69, no. 5, pp. 758–762, 2005.

[14] T. Yoshida, S. Takeyama, Y. Yamada, and K. Mutoh, "Nanometer-sized silicon crystallites prepared by excimer laser ablation in constant pressure inert gas," *Applied Physics Letters*, vol. 68, no. 13, pp. 1772–1774, 1996.

[15] X. Y. Chen, Y. F. Lu, Y. H. Wu et al., "Mechanisms of photoluminescence from silicon nanocrystals formed by pulsed-laser deposition in argon and oxygen ambient," *Journal of Applied Physics*, vol. 93, no. 10, pp. 6311–6319, 2003.

[16] Y. He, C. Yin, G. Cheng, L. Wang, X. Liu, and G. Y. Hu, "The structure and properties of nanosize crystalline silicon films," *Journal of Applied Physics*, vol. 75, no. 2, pp. 797–803, 1994.

[17] A. L. Patterson, "The scherrer formula for X-ray particle size determination," *Physical Review*, vol. 56, no. 10, pp. 978–982, 1939.

[18] K. Gouriet, L. V. Zhigilei, and T. E. Itina, "Molecular dynamics study of nanoparticle evolution in a background gas under laser ablation conditions," *Applied Surface Science*, vol. 255, no. 10, pp. 5116–5119, 2009.

[19] W. T. Nichols, G. Malyavanatham, D. E. Henneke et al., "Gas and pressure dependence for the mean size of nanoparticles produced by laser ablation of flowing aerosols," *Journal of Nanoparticle Research*, vol. 2, no. 2, pp. 141–145, 2000.

[20] Y. Wang, Y. Li, and G. Fu, "Relation between size-distribution of Si nanoparticles and oscillation-stabilization time of the mixed region produced during laser ablation," *Nuclear Instruments and Methods in Physics Research B*, vol. 252, no. 2, pp. 245–248, 2006.

[21] T. Makimura, T. Mizuta, T. Takahashi, and K. Murakami, "In situ size measurement of Si nanoparticles and formation dynamics after laser ablation," *Applied Physics A*, vol. 79, no. 4-6, pp. 819–821, 2004.

[22] S. S. Harilal, C. V. Bindhu, M. S. Tillack, F. Najmabadi, and A. C. Gaeris, "Internal structure and expansion dynamics of laser ablation plumes into ambient gases," *Journal of Applied Physics*, vol. 93, no. 5, pp. 2380–2388, 2003.